

Vegetation effects on impulsive events in the acoustic signature of fires

Kara M. Yedinak^{a)}

Department of Forest, Rangeland, and Fire Sciences, University of Idaho, 975 West 6th Street, Moscow, Idaho 83844, USA

Michael J. Anderson

Department of Mechanical Engineering, University of Idaho, 875 Perimeter Drive, Moscow, Idaho 83844, USA

Kent G. Apostol^{b)}

Department of Forest, Rangeland, and Fire Sciences, University of Idaho, 975 West 6th Street, Moscow, Idaho 83844, USA

Alistair M. S. Smith

Idaho Fire Initiative for Research and Education (IFIRE), 1025 Plant Science Road, Moscow, Idaho 83843, USA

(Received 4 November 2016; accepted 4 January 2017; published online 26 January 2017)

Acoustic impulse events have long been used as diagnostics for discrete phenomena in the natural world, including the detection of meteor impacts and volcanic eruptions. Wildland fires display an array of such acoustic impulse events in the form of crackling noises. Exploratory research into the properties of these impulse events revealed information regarding the specific properties of plant material. Unique acoustic frequency bands in the upper end of the sonic spectrum correlated to changes in vegetation properties. The signature of acoustic impulse events as they relate to plant species and plant water stress, were investigated in controlled laboratory combustion experiments. Correlation in the frequency range of 6.0–15.0 kHz was found for both species and water stress, indicating the possibility that a digital filter may be capable of identifying vegetation properties during wildland fire events. © 2017 Acoustical Society of America.

[<http://dx.doi.org/10.1121/1.4974199>]

[JFL]

Pages: 557–562

I. INTRODUCTION

Achieving a detailed understanding of open flame combustion in wildfires is of fundamental importance to physics and engineering, while at the same time, wildfires are under intense public scrutiny given the direct impacts on human health, safety, and property (Bowman *et al.*, 2009). Equally, early-warning indicators that aid in the near real-time assessment of ecosystem vulnerability to fires, such as from inferred vegetation properties, are critical to predict fire impacts on ecosystem goods and services (Carpenter *et al.*, 2011; Smith *et al.*, 2014).

Historically, open flame combustion has been evaluated using thermocouples or sensors attuned to the visible and thermal regions of the electromagnetic spectrum (Kremens *et al.*, 2010). Thermocouples and similar witness devices are often restricted by response times (Bova and Dickinson, 2009; Wotton *et al.*, 2012). The choice of visible and thermal radiometers can result in quantification challenges when the intervening space between the sensor and the wildfire is obscured by factors such as smoke, brush, or topography. Further, the high variability of combustion dynamics within

wildfires poses significant challenges in quantifying the fire behavior metrics of these phenomena (Keeley, 2009). This is due, in part, to the complexity of the burning vegetation, including variability associated with mortality, moisture level, quantity of vegetation, and plant species (Bigler *et al.*, 2005; Jolly, 2007; Keane, 2013; Matthews, 2014). To overcome these challenges, there is interest in the use of wildfire acoustics to aid in characterization of fire behavior (Bedard and Nishiyama, 2002; Sahin and Ince, 2009; Stavrakakis *et al.*, 2014; Viegas *et al.*, 2008).

A recent study found evidence of thermoacoustic and aeroacoustic phenomena in the 0–2 kHz range (Stavrakakis *et al.*, 2014). Another study found shrub fires exhibit an acoustic spectrum with decreasing amplitude as frequency increased from 0 to 500 Hz followed by amplitude increasing with frequency in the range 500 Hz–10 kHz (Viegas *et al.*, 2008). The increasing amplitude at higher frequencies was attributed to “crackling noises” during combustion. A compelling question that remains is whether the changing properties of the vegetation under combustion can be inferred from real-time sampling of the wildland fire combustion acoustics.

We hypothesize that the nature of “crackling noises,” i.e., short impulsive acoustic events during combustion, are affected by the species and presence of moisture in the vegetation being burned. For example, flash evaporation of liquid

^{a)}Electronic mail: kyedinak@uidaho.edu

^{b)}Current address: Central and Eastern Klickitat Conservation District, 1107 South Columbus Avenue, Goldendale, Washington 98620, USA.

mechanically contained in the vegetation is a likely cause of the short acoustic impulse events (AIEs). Then, it may be expected that the nature of the AIEs is affected by mechanical properties of the moisture containment and amount of moisture present in the vegetation. Elsewhere, AIEs have been successfully used as diagnostics for identifying unique events (Brown *et al.*, 2013; Hoffmann *et al.*, 1999; Abel *et al.*, 2010; ReVelle, 1976; Volgyesi *et al.*, 2007).

II. EXPERIMENTAL DESIGN

To investigate this hypothesis, we conducted laboratory experiments by burning conifer needles and whole seedlings. Two conifer seedling species were subjected to differing levels of water stress for 2 weeks prior to the combustion experiments. Acoustic measurements were recorded throughout the entire combustion process. AIEs attributed to the combustion of the conifer seedlings were isolated in 4 ms time segments. These segments were carefully selected to ensure no artifacts, i.e., acoustic reflections from the laboratory surroundings, were present in the signal of the AIE. Phase-contamination was also prevented by ensuring only one AIE was present in each time segment. Difference in means analysis of the spectra as well as an unbalanced analysis of variance (ANOVA) of individual AIEs was then performed to determine whether there was any correlation between the spectra of AIEs and the species and water stress level of the conifer seedlings.

A. Seedlings and combustion setup

The conifer seedlings consisted of 32 container-grown (2.5 cm diameter and 16 cm deep, 66 mL), seven-month old seedlings of both Douglas-fir (*Pseudotsuga menziesii* [Mirb.] Franco) and Engelmann spruce (*Picea engelmannii* Parry ex Engelm.). These seedlings were equally split and subjected to one of two moisture stress levels: well-watered (control), receiving water at 90% container capacity; or drought-stressed, receiving water at 65% container capacity for 2 weeks.

A 1.10 m long \times 1.30 m wide fuel bed of western white pine (*Pinus monticola* Douglas ex D. Don) needles with a fuel loading of 300 g m^{-2} was constructed (Fig. 1). Needles were collected from a single-species western white pine stand, manually sorted to remove impurities, and dried in an

oven at 90°C for 24 h to bring them to 0% fuel moisture content. A fuel bed was made up of western white pine needles and either eight Douglas-fir or Engelmann spruce seedlings placed 18 cm apart linearly and parallel to the ignition which was 74 cm from the seedlings. Each burn contained only one conifer seedling species and one moisture stress level. The seedling culture and growing conditions were carefully monitored (Apostol *et al.*, 2015). Two burns were conducted for each of the two moisture stress levels for each species.

The branch water potential was measured on all seedlings 1 day before the experiment using a model 600 Pressure Chamber (PMS Instruments Company, Albany, OR, USA). Shoot moisture content was calculated as the difference between tissue fresh mass (FM) and dry mass (DM) after oven-drying at 70°C for 72 h.

The experiments took place at the Idaho Fire Initiative for Research and Education combustion laboratory located at the University of Idaho. This laboratory is a steel-sided building with approximate lateral inside dimensions of $7.3 \text{ m} \times 5.5 \text{ m}$, a peaked ceiling with heights varying from 3.3 m at the sides to 4.0 m in the center, and a cement floor. Laboratory equipment was located along the walls. The nearest structure was a polyhedron shaped vent hood located $\sim 1 \text{ m}$ above the experiment. To minimize the effects of conductive heat transfer, the burns took place on a fire-brick lined table ($1.30 \text{ m long} \times 1.43 \text{ m wide} \times 0.92 \text{ m tall}$). A continuous flame front progressed through the pine needles, encountered and combusted the conifer seedlings, and terminated at the far end of the fuel bed. The flame front was nominally parallel to the linear array of seedlings, and perpendicular to the axis of the microphone. The microphone signals show, in order of occurrence, an ignition, combustion of pine needles, ignition and combustion of conifer seedlings with pine needles, and combustion of pine needles until termination (Figs. 2A–2D).

B. Acoustic measurement setup

During the combustion process, a $1/2 \text{ in.}$ diameter pressure-response (Wong and Embleton, 1994) measurement microphone (Bruel & Kjaer, type 4134), positioned near the edge of the fuel bed, was used to record the acoustic signal. The microphone was placed $\sim 1 \text{ m}$ from the center, 6.5 cm from the ignition point, and at an elevation of $\sim 23 \text{ cm}$ above



FIG. 1. (Color online) Fuels and fuel bed setup before, during, and post fire. (A) Flame front (indicated by dotted black line) moves in the direction of the black arrow towards conifer seedlings (denoted by green dashed arrows). (B) Side view of the experimental setup shows the configuration of the free field microphone and camera (far left), the location and extent of the linear ignition (yellow dashed line) along the left edge of a pine needle fuel bed with conifer seedlings in position in the last quarter (right side) of the fuel bed. (C) Conifer seedlings, post combustion, show charring and damage to green needles. Bricks in background included for image clarity.

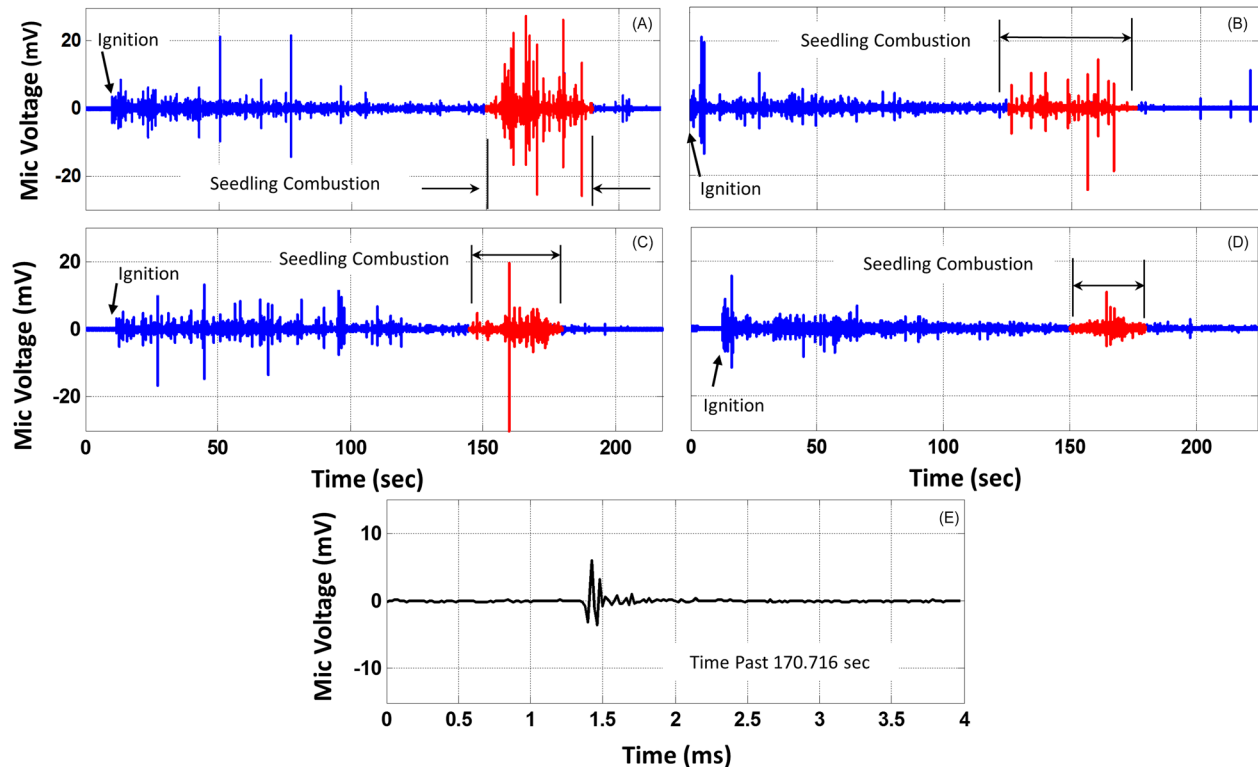


FIG. 2. (Color online) Microphone voltage during combustion of conifer seedlings. Left column [(A) and (C)]: water-stressed, right column [(B) and (D)]: well-watered. First row [(A) and (B)]: Engelmann spruce, second row [(B) and (E)]: Douglas-fir, third row (E): selected AIE during seedling burn.

the plane of the fuel materials on the table. The microphone was a pressure-response type, nominal sensitivity of 9 mV Pa^{-1} as determined by a piston-phone, and bandwidth 20 Hz–25 kHz. The microphone signal was alias-filtered, amplified, and digitized at a rate of 50 kHz with 12 bit resolution. After digitization, a high-pass digital filter, with a corner frequency of 10 Hz was applied to the microphone signal to remove slowly varying electronic noise.

The measurement environment was not anechoic, thus it is assumed that the acoustic measurements contained reflective artifacts from surrounding walls, roof, floor, and obstacles. Aside from the table supporting the experiment, the nearest reflective surface (laboratory vent hood) was $\sim 1 \text{ m}$ away (echo-return time $> 5.8 \text{ ms}$). During all experiments, combustion was initiated near the microphone at the edge of the fuel bed (Fig. 1).

III. EXPERIMENTAL RESULTS

A. Statistical analysis of seedling moisture stress

An ANOVA was performed with a Tukey's test to compare moisture means for significant differences ($p\text{-value} < 0.05$). Both branch water potential (Ψ_w) and shoot moisture content in Douglas-fir and Engelmann spruce significantly decreased with drought induced moisture stress. Mean Ψ_w values in the well-watered and drought-stressed Douglas-fir and Engelmann spruce seedlings were -1.3 , -3.5 , -1.7 , and -4.1 MPa , respectively. Shoot moisture content values in the well-watered and drought-stressed Douglas-fir and Engelmann spruce seedlings were 0.7 , 0.5 , 0.5 , and 0.4 g , respectively.

B. AIE magnitude

In the plots of microphone voltage [Figs. 2(A)–2(E)], a time-segment (annotated as “seedling combustion”) was selected corresponding to the combustion of seedlings. The microphone voltage magnitude during seedling combustion varied between seedling moisture levels and, to a lesser degree, between species. For example, the microphone voltage magnitude was larger for the drought-stressed seedlings of both species [Figs. 2(A) and 2(C)] when compared to those that were well-watered [Figs. 2(B) and 2(D)]. Likewise, the microphone voltage magnitude was larger during Engelmann spruce seedling burns [Figs. 2(A) and 2(B)] as compared to the Douglas-fir seedling burns [Figs. 2(C) and 2(D)].

C. Average normalized spectrum of AIEs

In addition to the amplitude of individual AIEs, we investigated whether an amplitude-independent signature could be associated with seedling conditions. Individual AIEs associated with the burning seedlings were isolated by selecting 4 ms time segments, during seedling combustion, which contained a single large-magnitude AIE [Fig. 2 (E)]. This procedure likely isolates AIEs caused by seedlings because (1) the AIEs caused by seedlings were higher in magnitude than those caused by the pine needle fuel bed and (2), a 4 ms duration excludes the possibility of propagation of AIE reflections from the surrounding environment (objects $> 1 \text{ m}$ away equates to an echo-return time $> 5.8 \text{ ms}$).

In total, 361 AIEs associated with seedling combustion were isolated. The normalized spectrum of each AIE was obtained by dividing the power at each frequency by the

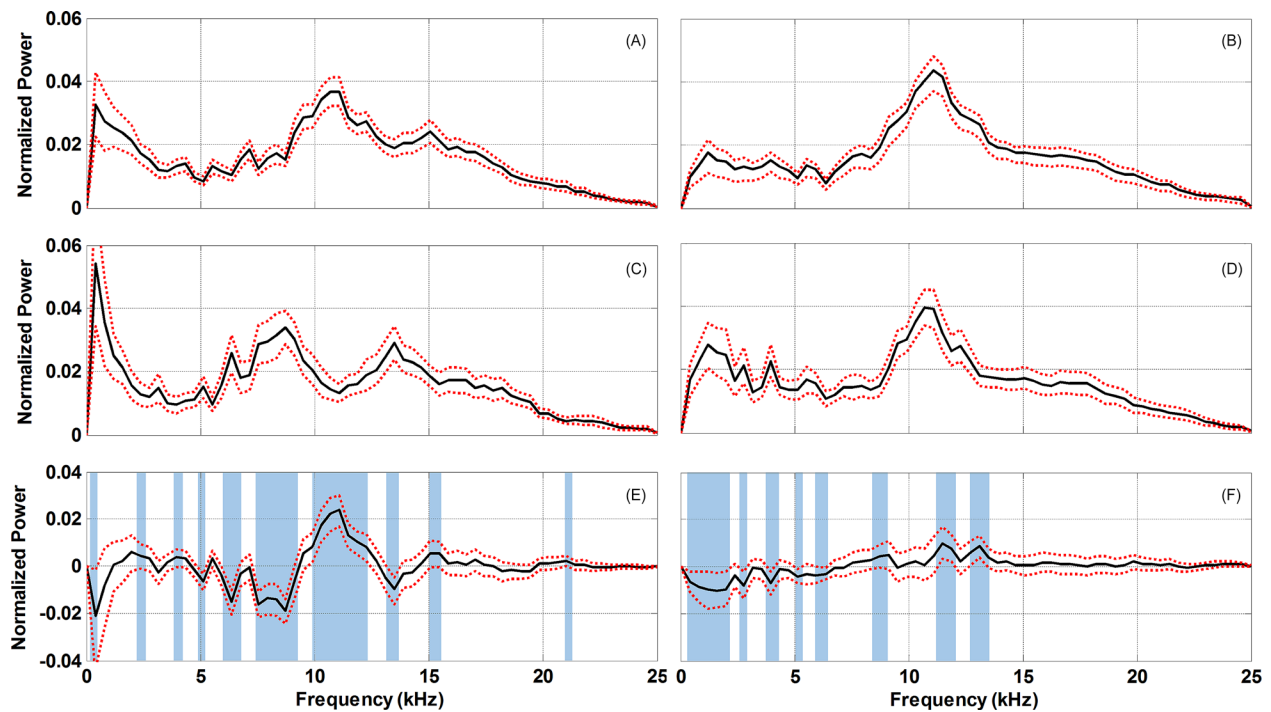


FIG. 3. (Color online) Water-stress difference quantification using normalized power of AIEs during combustion of conifer seedlings. Left column [(A)–(E)]: Douglas-fir, right column [(B)–(F)]: Engelmann spruce. First row [(A) and (B)]: mean (solid line) normalized spectrum of water-stressed seedling AIEs during combustion with 95% confidence interval (dashed line), second row [(C) and (D)]: mean (solid line) normalized spectrum of well-watered seedling AIEs during combustion with 95% confidence interval (dashed line), third row: difference in means of the average normalized spectrum of AIEs for Douglas-fir changes in water-stress level (E) and Engelmann spruce changes in water-stress level (F). Shaded (blue) areas indicate the wavelength ranges for which a change in water stress produced significantly different acoustic signatures.

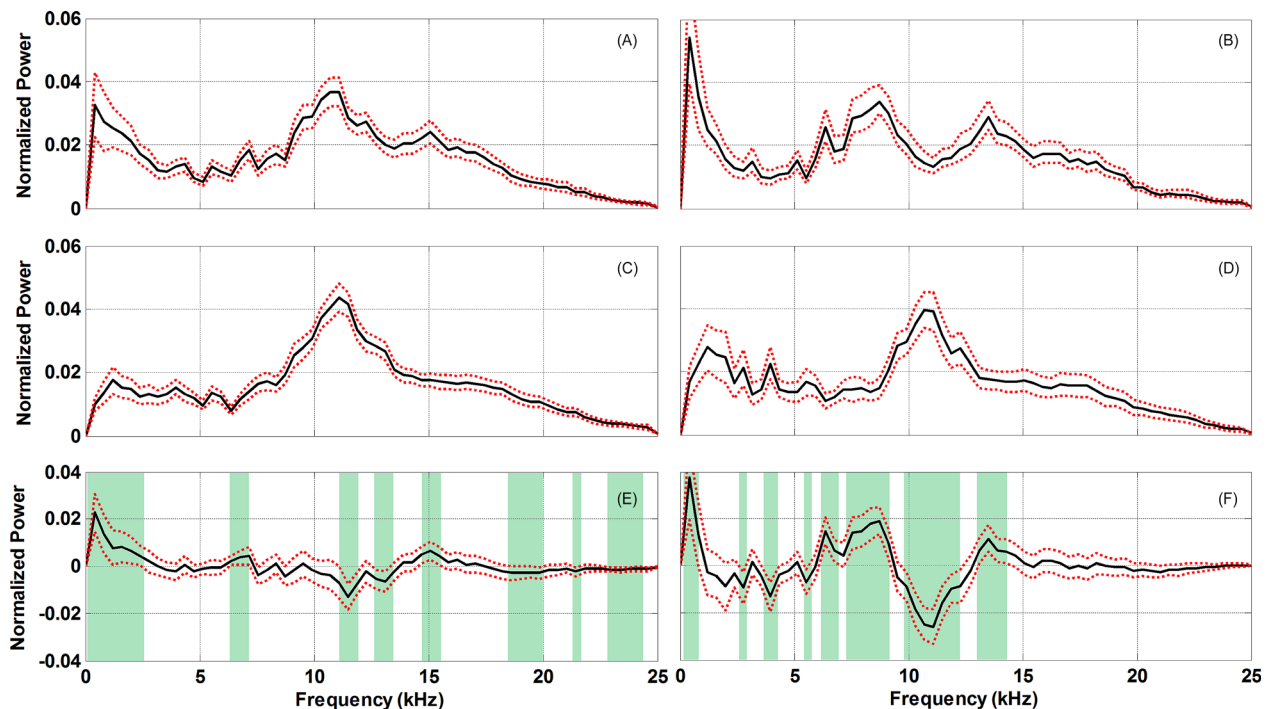


FIG. 4. (Color online) Species difference quantification using normalized power of AIEs during combustion of conifer seedlings. Left column [(A)–(E)]: water-stressed, right column [(B)–(F)]: well-watered. First row [(A) and (B)]: mean (solid line) normalized spectrum of Douglas-fir AIEs during combustion with 95% confidence interval (dashed line), second row [(C) and (D)]: mean (solid line) normalized spectrum of Engelmann spruce AIEs during combustion with 95% confidence interval (dashed line), third row: difference in means of the average normalized spectrum of AIEs for water-stressed changes in species (E) and well-watered changes in species (F). Shaded (green) areas indicate the wavelength ranges for which a change in species produced significantly different acoustic signatures.

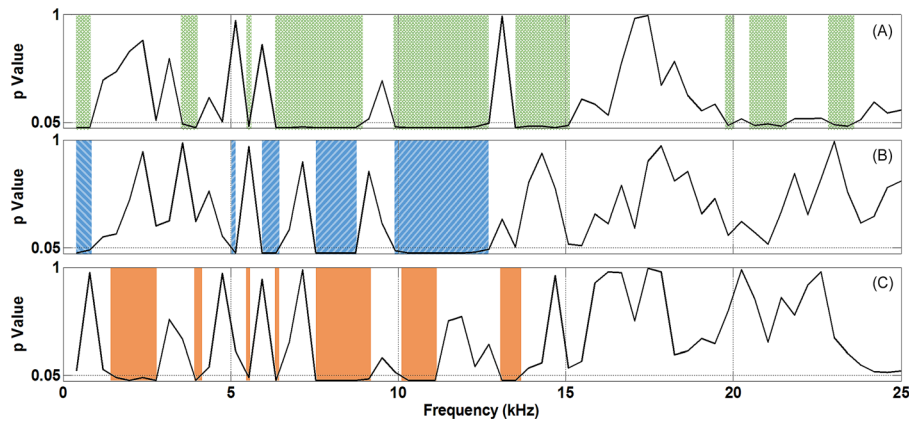


FIG. 5. (Color online) Two-factor unbalanced ANOVA analysis of the average normalized spectrum of AIEs at each frequency. Vertical axis contains p-value for (A) species, (B) water-stress, and (C) species/water-stress interaction. The shaded areas indicate regions within the frequency range in which species (top panel), water-stress (middle panel), or their interaction (bottom panel) significantly (p -value < 0.05) influenced the AIE averaged normalized spectrum.

overall power in the microphone voltage signal during the duration of seedling combustion. A free-field correction factor, provided by the manufacturer, for a plane wave incident at 0° to the microphone axis was applied to the spectrum to correct for microphone diffraction (Matsui, 1971). An average normalized spectrum was then computed from the 361 isolated AIEs for each of the four combinations of species and water stress [Figs. 3 and 4(A)–4(D)].

Initial inspection of the AIE spectra [Figs. 3 and 4(E) and 4(F), shaded areas], shows some dependence of the spectra on species. When Engelmann spruce was combusting, a single peak (~ 12 kHz) occurred in the average normalized spectrum [Figs. 3(B) and 3(D)]. When the Douglas-fir seedlings were combusting [Figs. 3(A) and 3(C)] the average normalized spectrum changed to a two-peak structure, with separate peaks at ~ 11 and 15 kHz for the water-stressed seedlings and ~ 8 and 13 kHz for well-watered seedlings. A 95% confidence interval, for the difference in means in the averaged normalized spectrum of each frequency, revealed that the difference for water stress was non-zero, and thus statistically significant (p -value < 0.05) for both species [Figs. 3(E) and 3(F), shaded regions]. A two-factor unbalanced ANOVA of the same average normalized spectrum at each frequency supported and further refined these results indicating AIEs were significantly sensitive (p -value < 0.05) to changes in water stress in five separate frequency bands between ~ 0.4 and 13 kHz [Fig. 5(B), shaded regions].

Differences in the average normalized spectrum between species were also detected. When each species was water-stressed, a difference in means test revealed a statistically significant (p -value < 0.05) difference in the average normalized spectrum in eight separate regions spanning the entire sampling frequency range [Fig. 4(E), shaded green]. Likewise, when both species were well-watered [Fig. 4(F), shaded green], a statistically significant (p -value < 0.05) difference in average spectra was observed in the frequency range ~ 0.40 – 14.5 kHz. A two-factor unbalanced ANOVA of the same data gave similar but more refined results indicating AIEs were significantly sensitive (p -value < 0.05) to changes in species in nine frequency bands between 0.40 and 23.5 kHz [Fig. 5(A)]. The two largest frequency bands sensitive to species differences, from ~ 6 – 9 kHz and ~ 10 – 13 kHz [Fig. 5(A)], are likely due to a low point at ~ 12 kHz in the average normalized spectra for well-watered Douglas-fir [Fig. 4(B)]

and a corresponding peak in the average normalized spectra [Fig. 4(D)] for well-watered Engelmann spruce.

The authors have less confidence in correlations at low frequencies, due to omnidirectional scattering of sound from surrounding structures, whereas scattering at high frequencies is more directed in nature. Interactions between water-stress and species were found in seven frequency bands between ~ 1.5 and 13.5 kHz [Fig. 5(C)]. Three regions of interaction 6.30 kHz, 7.54 – 9.20 kHz, and 10.0 – 11.1 kHz correspond with sensitivity to both species and water-stress.

IV. CONCLUSIONS

A surprising degree of correlation in AIEs was observed to be associated with species and water-stress level in the frequency range ~ 6.0 – 15 kHz. AIE analysis for species also revealed strong correlation between ~ 20.0 and 23.5 kHz. Several specific regions within these frequency regions were found to be unique to either water-stress level (5.15 and 6.00 – 6.30 kHz) or species (6.35 – 7.54 , 13.5 – 15.0 , 19.8 , 20.6 – 21.5 , and 23.0 – 23.6 kHz). The identification of acoustic wavelength bands sensitive to changes in plant species and plant water-stress levels opens the door for development of inexpensive digital acoustic filters allowing for characterization of real-time properties of vegetation involved in wildland fires. For example, it may be possible to detect the type and moisture-stress level of vegetation burning at any given time during a wildland fire, a feat not currently possible without prior knowledge of the local environment. A more comprehensive set of studies encompassing a wider breadth of plants is needed to fully understand the unique acoustic signatures of individual species. This study illustrates the merits of acoustic sampling of wildland fire events and provides a solid foundation for development of wildland fire acoustics research.

ACKNOWLEDGMENTS

The present research was supported in part by funds provided by the USDA Forest Service (Grant No. 15-JV-11261987-082) and the National Science Foundation (Grant No. DMS-1520873). We thank the United States funding agencies, research centers, and participants who made this research possible: the Wildland Fire Science Partnership; the USDA Forest Service Rocky Mountain Research Station; the

University of Idaho, College of Natural Resources Center for Forest Nursery and Seedling Research; the University of Idaho, Department of Mechanical Engineering; Dr. Owen Burney and the USDA Forest Service Coeur d'Alene Nursery for providing seeds. We also thank Amanda Argona, Wade Tinkham, Sally Mei, and Leslie Fowler for their technical help.

- Abel, J. S., Bryan, N. J., Huang, P. P., Kolar, M. A., and Pentcheva, B. V. (2010). "Estimating room impulse responses from recorded balloon pops," Presented at the *129th AES Convention*, Audio Engineering Society, San Francisco, CA, USA.
- Apostol, K. G., Dumroese, R. K., Pinto, J. R., and Davis, A. S. (2015). "Response of conifer species from three latitudinal populations to light spectra generated by light-emitting diodes and high-pressure sodium lamps," *Can. J. For. Res.* **45**, 1711–1719.
- Bedard, A. J., and Nishiyama, R. T. (2002). "Infrasound generation by large fires: Experimental results and a review of an analytical model predicting dominant frequencies," presented at the *Geoscience and Remote Sensing Symposium, 2002, IGARSS'02*, IEEE International, 2002, Vol. 2, pp. 876–878.
- Bigler, C., Kulakowski, D., and Veblen, T. T. (2005). "Multiple disturbance interactions and drought influence fire severity in rocky mountain subalpine forests," *Ecology* **86**, 3018–3029.
- Bova, A. S., and Dickinson, M. B. (2009). "An inverse method to estimate stem surface heat flux in wildland fires," *Int. J. Wildland Fire* **18**, 711–721.
- Bowman, D. M. J. S., Balch, J. K., Artaxo, P., Bond, W. J., Carlson, J. M., Cochrane, M. A., D'Antonio, C. M., DeFries, R. S., Doyle, J. C., Harrison, S. P., Johnston, F. H., Keeley, J. E., Krawchuk, M. A., Kull, C. A., Marston, J. B., Moritz, M. A., Colin Prentice, I., Roos, C. I., Scott, A. C., Swetnam, T. W., van der Werf, G. R., and Pyne, S. J. (2009). "Fire in the Earth system," *Science* **324**, 481–484.
- Brown, P. G., Assink, J. D., Astiz, L., Blaauw, R., Boslough, M. B., Borovička, J., Brachet, N., Brown, D., Campbell-Brown, M., Ceranna, L., Cooke, W., de Groot-Hedlin, C., Drob, D. P., Edwards, W., Evers, L. G., Garces, M., Gill, J., Hedlin, M., Kingery, A., Laske, G., Le Pichon, A., Mialle, P., Moser, D. E., Saffer, A., Silber, E., Smets, P., Spalding, R. E., Spurný, P., Tagliaferri, E., Uren, D., Weryk, R. J., Whitaker, R., and Krzeminski, Z. (2013). "A 500-kiloton airburst over Chelyabinsk and an enhanced hazard from small impactors," *Nature* **503**, 238–241.
- Carpenter, S. R., Cole, J. J., Pace, M. L., Batt, R., Brock, W. A., Cline, T., Coloso, J., Hodgson, J. R., Kitchell, J. F., Seekell, D. A., Smith, L., and Weidel, B. (2011). "Early warnings of regime shifts: A whole-ecosystem experiment," *Science* **332**, 1079–1082.
- Hoffmann, W., Kebeasy, R., and Firbas, P. (1999). "Introduction to the verification regime of the Comprehensive Nuclear-Test-Ban Treaty," *Phys. Earth Planet. Inter.* **113**, 5–9.
- Jolly, W. M. (2007). "Sensitivity of a surface fire spread model and associated fire behaviour fuel models to changes in live fuel moisture," *Int. J. Wildland Fire* **16**, 503–509.
- Keane, R. E. (2013). "Describing wildland surface fuel loading for fire management: A review of approaches, methods and systems," *Int. J. Wildland Fire* **22**, 51–62.
- Keeley, J. E. (2009). "Fire intensity, fire severity and burn severity: A brief review and suggested usage," *Int. J. Wildland Fire* **18**, 116–126.
- Kremens, R. L., Smith, A. M. S., and Dickinson, M. B. (2010). "Fire metrology: Current and future directions in physics-based measurements," *Fire Ecol.* **6**, 13–35.
- Matsui, E. (1971). "Free-field correction for laboratory standard microphones mounted on a semiinfinite rod," *J. Acoust. Soc. Am.* **49**, 1475–1483.
- Matthews, S. (2014). "Dead fuel moisture research: 1991–2012," *Int. J. Wildland Fire* **23**, 78–92.
- ReVelle, D. O. (1976). "On meteor-generated infrasound," *J. Geophys. Res.* **81**, 1217–1230, doi:10.1029/JA081i007p01217.
- Sahin, Y. G., and Ince, T. (2009). "Early forest fire detection using radio-acoustic sounding system," *Sensors* **9**, 1485–1498.
- Smith, A. M. S., Kolden, C. A., Tinkham, W. T., Talhelm, A. F., Marshall, J. D., Hudak, A. T., Boschetti, L., Falkowski, M. J., Greenberg, J. A., Anderson, J. W., Kliskey, A., Alessa, L., Keefe, R. F., and Gosz, J. R. (2014). "Remote sensing the vulnerability of vegetation in natural terrestrial ecosystems," *Remote Sens. Environ.* **154**, 322–337.
- Stavrakakis, P., Agapiou, A., Miki, K., Karma, S., Statheropoulos, M., Pallis, G. C., and Pappa, A. (2014). "A scale-up field experiment for the monitoring of a burning process using chemical, audio, and video sensors," *Environ. Sci. Pollut. Res.* **21**, 891–900.
- Viegas, D. X., Pita, L. P., Nielsen, F., Haddad, K., Tassini, C. C., D'Altrui, G., Quaranta, V., Dimino, I., and Hao, W. M. (2008). "Acoustic and thermal characterization of a forest fire event," in *Remote Sensing of Fire: Science and Application*, edited by W. M. Hao, SPIE—International Society of Optical Engineering, Bellingham, Vol. 7089, p. 708904.
- Volgyesi, P., Balogh, G., Nadas, A., Nash, C. B., Ledecz, A., Simon, G., Fehér, B., and Dóra, S. (2007). "Shooter localization and weapon classification with soldier-wearable networked sensors," in *The 5th ACM International Conference on Mobile Systems, Applications, and Services, MobiSys, 2007*.
- Wong, G. S. K., and Embleton, T. E. W. (1994). *AIP Handbook of Condenser Microphones: Theory, Calibration and Measurements* (American Institute of Physics, New York).
- Wotton, B. M., Gould, J. S., McCaw, W. L., Cheney, N. P., and Taylor, S. W. (2012). "Flame temperature and residence time of fires in dry eucalypt forest," *Int. J. Wildland Fire* **21**, 270–281.